

Proteogenomic Analysis of a Hibernating Mammal Indicates Contribution of Skeletal Muscle Physiology to the Hibernation Phenotype

Kyle J. Anderson,[†] Katie L. Vermillion,[†] Pratik Jagtap,^{‡,§} James E. Johnson,^{||} Timothy J. Griffin,^{‡,§} and Matthew T. Andrews^{*,†}

[†]Department of Biology, University of Minnesota Duluth, 1035 Kirby Drive, Duluth, Minnesota 55812, United States

[‡]Center for Mass Spectrometry and Proteomics, University of Minnesota, 1479 Gortner Avenue, St. Paul, Minnesota 55108, United States

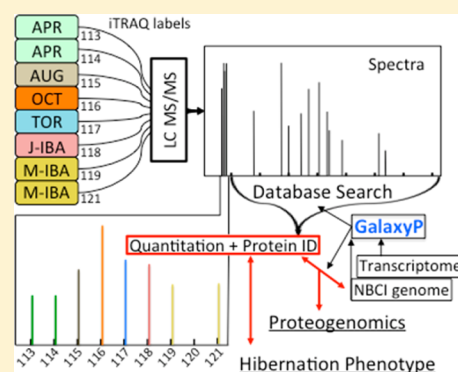
[§]Department of Biochemistry, Molecular Biology, and Biophysics, University of Minnesota, 321 Church Street South East, Minneapolis, Minnesota 55455, United States

^{||}Minnesota Supercomputing Institute, 512 Walter Library, 117 Pleasant Street South East, Minneapolis, Minnesota 55455, United States

Supporting Information

ABSTRACT: Mammalian hibernation is a strategy employed by many species to survive fluctuations in resource availability and environmental conditions. Hibernating mammals endure conditions of dramatically depressed heart rate, body temperature, and oxygen consumption yet do not show the typical pathological response. Because of the high abundance and metabolic cost of skeletal muscle, not only must it adjust to the constraints of hibernation, but also it is positioned to play a more active role in the initiation and maintenance of the hibernation phenotype. In this study, MS/MS proteomic data from thirteen-lined ground squirrel skeletal muscles were searched against a custom database of transcriptomic and genomic protein predictions built using the platform Galaxy-P. This proteogenomic approach allows for a thorough investigation of skeletal muscle protein abundance throughout their circannual cycle. Of the 1563 proteins identified by these methods, 232 were differentially expressed. These data support previously reported physiological transitions, while also offering new insight into specific mechanisms of how their muscles might be reducing nitrogenous waste, preserving mass and function, and signaling to other tissues. Additionally, the combination of proteomic and transcriptomic data provides unique opportunities for estimating post-transcriptional regulation in skeletal muscle throughout the year and improving genomic annotation for this nonmodel organism.

KEYWORDS: *i*TRAQ, *Galaxy-P*, proteogenomics, hibernation, skeletal muscle, AMP – deaminase 1, fibromodulin, quantitative proteomics



INTRODUCTION

In seasonal environments many mammalian species employ the energy-conserving strategy of hibernation to survive the annual waning of resources in the winter months. For many obligate small mammal hibernators such as the thirteen-lined ground squirrel (*Ichthyomys tridecemlineatus*), hibernation is characterized by long bouts of torpor (TOR) that are interrupted by shorter interbout arousals (IBA).¹ Torpid ground squirrels display dramatically reduced metabolic rates, with body temperatures (T_b) dipping to near-ambient (T_a) (4–10 °C), oxygen consumption as low as 2 to 3% of euthermic levels, and a heart rate of 3–10 bpm versus an active rate of 300–400 bpm.^{1,2} They remain in this motionless state for 7–10 days before rewarming for periodic IBAs. During an IBA the squirrels maintain normal physiological parameters for 12–24 h

before once again reducing their metabolism and allowing their body to passively cool for another bout of torpor. This cycle is repeated numerous times throughout the hibernation season. During these 4–6 months, the squirrels cease food consumption and derive energy from lipid stores accumulated throughout the rest of the year.

Given the high abundance and metabolic demand of skeletal muscle, it seems reasonable that this tissue would not only have major challenges overcoming the physiological transitions associated with hibernation but also contribute significantly to making these transitions possible on a whole-organism level. Skeletal muscle comprises ~40% of the total mass of most

Received: December 17, 2015

Published: February 23, 2016

mammalian species including humans and is responsible for 20–30% of resting metabolic demand.³ Additionally, the high plasticity of skeletal muscle in response to metabolic and functional demands makes it an ideal target for hibernators to adjust whole-body physiological parameters with the alteration of a single tissue.^{4,5} The structural, functional, and metabolic properties of skeletal muscle fibers tend to differentiate together in such a way that muscle fibers can generally be classified on a spectrum from slow to fast fiber types and will have more oxidative or glycolytic metabolic properties, respectively.⁶ Extended disuse in nonhibernating mammals results in a slow to fast muscle type transition, resulting in a more glycolytic metabolism;⁷ however, hibernator muscles undergo a fast to slow transition leading up to hibernation and maintain that fiber-type distribution until the spring.⁸ This fiber-type maintenance is partly explained by activation of the exercise endurance pathway and the activity of the transcriptional coactivator PGC-1 α .⁹ By transitioning to a slower fiber type prior to hibernation, not only are their muscles primed to utilize fatty acids as the primary fuel source but also activation of this pathway likely contributes to their seeming resistance to disuse atrophy.⁹

Maintaining contractile function despite extended disuse is another important demand placed on hibernator skeletal muscle. During an arousal, the T_b of a squirrel changes from only a few degrees above freezing to 37 °C in ~2 h. The initial stages of this rewarming are mediated by nonshivering thermogenesis in brown adipose tissue (BAT), while the later stages also make use of shivering thermogenesis in skeletal muscle.¹⁰ In the spring, these hibernators arouse to an environment full of predatory mammals and birds that are hungry after a long winter or migration. Functional muscles are essential to forage, evade predation and successfully reproduce. Despite extended winter disuse, these animals' muscles seem to be fully functional at the conclusion of hibernation.^{11,12} In addition to the potential effects of PGC-1 α expression, a variety of mechanisms have been proposed to maintain hibernator muscle. Andres-Mateos et al. demonstrated the role of serum/glucocorticoid-induced kinase in maintaining protein synthesis/degradation balance in hibernation.¹¹ Various research groups have demonstrated a decrease in protein abundance of myostatin, a negative regulator of muscle mass, during the bulk of hibernation.^{12,13} Another hypothesis, one supported by this data, is that these animals undergo a period of muscle growth during the final stages of hibernation, in preparation for the final spring arousal.¹⁴

To better understand skeletal muscle function throughout this complex annual cycle and how it might contribute to the hibernation phenotype, we performed a shotgun proteomics screen with iTRAQ labeling, allowing us to quantify skeletal muscle protein abundance at six time points throughout the year. Using a proteogenomic approach described in a similar study from our lab,¹⁵ the tools within data analysis platform Galaxy-P^{16–18} were used to create a custom protein sequence database by combining predicted protein sequences from RNAseq data and the NCBI thirteen-lined ground squirrel genome. This in-depth method identified over 1500 proteins, of which 232 were differentially expressed. Using both RNAseq and peptide sequence data, we identified protein sequences not predicted in the NCBI genome. These novel sequences improve annotation of the thirteen-lined ground squirrel genome and could be derived from novel proteoforms¹⁹ important to the hibernation phenotype. By comparing

transcript expression to their respective proteins, the data suggest different levels of post-transcriptional regulation throughout the year. Trends in protein abundance support well-known hibernator muscle physiology, such as the reliance on lipids for energy^{1,2,15} and fiber-type switching,^{15,20} while also illustrating the time scale over which these transitions occur. The differential abundance of specific proteins, such as AMP deaminase-1 and fibromodulin, presents promising hypotheses that could expand our knowledge of the hibernation phenotype.

EXPERIMENTAL SECTION

Animal Models

Thirteen-lined ground squirrels (*ICTIDOMYS TRIDECIMLINEATUS*) used in this study were obtained and housed as previously described.^{15,20} All experimental animal procedures were approved by the University of Minnesota Institutional Animal Care and Use Committee. The following collection points served to reveal changes in protein abundance throughout the circannual cycle: April active (APR), August active (AUG), October active (OCT), January torpor (TOR), January interbout arousal (J-IBA), and March interbout arousal (M-IBA) (Figure 1). Three females and three males were collected

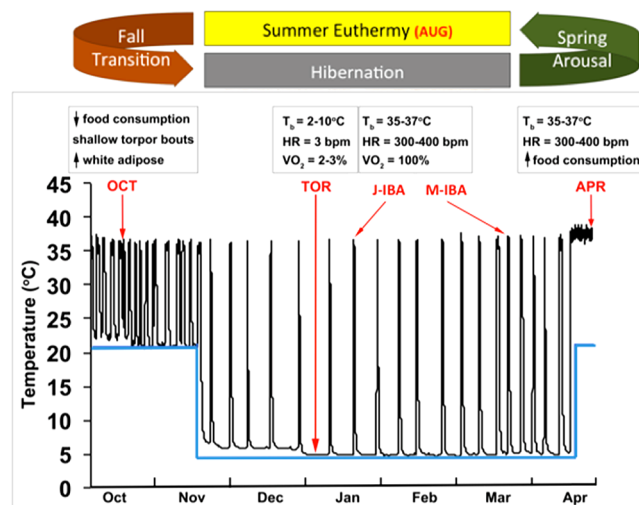


Figure 1. Circannual cycle of a thirteen-lined ground squirrel and tissue collection points. The black line represents the core body temperature (T_b) of a single animal measured by a surgically implanted transmitter. The blue line represents ambient temperature (T_a). Arrows indicate representative times and T_b at which animals were collected.

at each time point. A single female sample and a single male sample were eventually pooled to produce three samples comprising both sexes. Three mass spectrometry runs were performed on iTRAQ-labeled samples with each including one sample from each of the six time points. This resulted in a total of three biological replicates for each time point. Physiological state was determined by rectal temperature and animal behavior. At all time points, animals were anesthetized with isoflurane and sacrificed by decapitation. The quadriceps muscles were dissected and immediately frozen in liquid nitrogen and stored at -80 °C. Animals collected for all time points, except TOR, had a body temperature (T_b) of 35–37 °C and were observed as being fully awake and active prior to sacrifice. Torpid animals were collected after a minimum of 3

days of consecutive torpor, showed no outward signs of arousal, and had a T_b of 5–7 °C at the time of sacrifice.

Protein Extraction and iTRAQ Labeling

Frozen tissue was ground to a powder under liquid nitrogen. Tissue was reconstituted in extraction buffer (7 M urea, 2 M thiourea, 0.4 M triethylammonium bicarbonate (TEAB) pH8.5, 20% acetonitrile, and 4 mM Tris (2carboxyethyl) phosphine (TCEP)) at a ratio of 10 mL/g. While remaining on ice, the samples were sonicated with a Branson Digital Sonifier 250 at 30% amplitude for no more than seven consecutive seconds to avoid carbamylation. A volume of 150 μ L of each sample was transferred to a Pressure Cycling Technology tube and capped with a 150 μ L cap before being placed in the Barocycler NEP2320 (Pressure Biosciences, South Easton, MA). Samples underwent 40 cycles of 35 kpsi for 30 s, followed by 0 psi for 15 s. Following pressure cycling, 200 mM methylmethanesulfonate (MMS) was added to a final concentration of 8 mM, mixed, and incubated at room temperature for 15 min. Samples were then transferred to a new 1.5 mL microfuge Eppendorf Protein LoBind tube. Protein concentration was determined by Bradford assay.

Protein from a single male and a single female (50 μ g each) were pooled to produce samples of 100 μ g. This was brought up to a least common volume in protein extraction buffer and MMS. Samples were diluted 4-fold with ultrapure water, followed by the addition of trypsin (Promega, Madison, WI) at a ratio of 35:1 total protein to trypsin. Samples were incubated at 37 °C for 16 h and then frozen at –80 °C for 30 min prior to drying by vacuum centrifugation. After cleaning the samples using normal-phase solid-phase extraction (SPE) (Extract Clean C18 SPE cartridge, Grace-Davidson, Deerfield, IL), the eluents were vacuum-dried and resuspended in dissolution buffer (0.5 M TEAB pH8.5) to a final concentration of 2 μ g/ μ L. iTRAQ labeling was done per manufacturer's protocol (AB Sciex, Foster City, CA). After labeling, samples were multiplexed and vacuum-dried. Samples were cleaned by normal phase SPE as before and eluents were dried by vacuum centrifuge.

Liquid Chromatography Fractionation and Mass Spectrometry

Labeled samples were resuspended in Buffer A (20 mM ammonium formate pH 10 in 98:2 water/acetonitrile) and fractionated offline by high pH C18 reverse-phase chromatography.²¹ A Shimadzu Promenace HPLC (Shimadzu, Columbia, MD) was used with a C18 XBridge column, 150 mm \times 2.1 mm internal diameter, 5 μ m particle size (Walters Corporation, Milford, MA). Flow rate was 200 μ L/min with a gradient from 2 to 35% Buffer B (20 mM ammonium formate pH 10 in 10:90 water/acetonitrile) over 60 min, followed by 35–60% over 5 min. Fractions were collected every 2 min, and UV absorbances were monitored at 215 and 280 nm. Peptide-containing fractions were divided into early and late groups, each containing an equal number of fractions. The first early fraction was concatenated with the first late fraction and so on. Concatenated samples were dried by vacuum centrifugation and resuspended in load solvent (98:2:0.01 water/acetonitrile/formic acid), and 1 to 1.5 μ g aliquots were run on a Velos Orbitrap mass spectrometer (Thermo Fisher Scientific, Waltham, MA) as previously described with the exception that the higher-energy collisional dissociation activation energy was 20 ms.

Bioinformatic Analysis

MS/MS spectra were searched using a customized ground squirrel database.¹⁵ This database was generated using predicted protein sequences from the NCBI annotated genome for the thirteen-lined ground squirrel, RNaseq data generated in this lab,²⁰ and a contaminants database (cRAP) containing common or unavoidable MS protein contaminants. Databases were merged using tools within the Galaxy-P platform (University of Minnesota) and searched using Paragon Algorithm (V.4.5.0.0) search engine in Protein Pilot (V.4.5, Sciex, Foster City, CA) with the following search parameters: Sample Type: iTRAQ 8-plex (peptide labeled); Cys-alkylation: MMTS; Instrument: Orbi MS, Orbi MS/MS; Run Quant; Use bias correction; Search focus on biological modifications; Thorough search and with a Detected Protein Threshold (Unused Protscore (Conf)): 10%. The ProteinPilot searches and subsequent generation of PSPEP (FDR) reports and protein and peptide-level summaries were generated within Galaxy-P.

All peptides were identified with at least a 95% confidence interval value, as specified by the Paragon Algorithm and a <1% false discovery rate (FDR) based on forward and reverse searches. Proteins were considered confidently identified with at least two unique peptides and an experiment-wide FDR of no more than 2%. Relative quantification of proteins was determined by ProteinPilot. ProteinPilot begins quantitation at the level of the peptide by calculating a ratio of any 2 iTRAQ label peak intensities (Figure 2). Ratios from all peptides

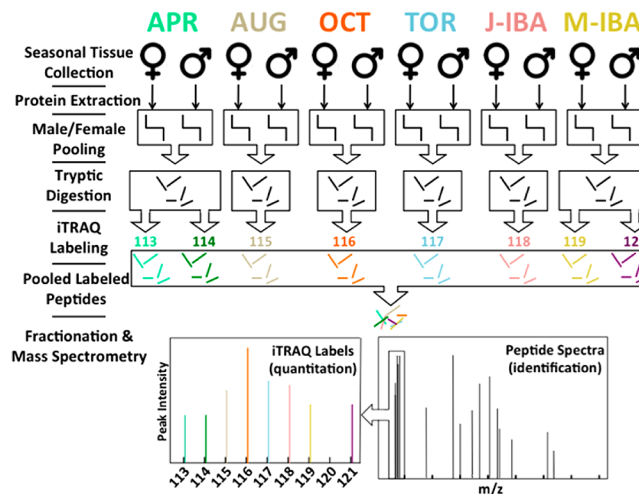


Figure 2. Sampling design, preparation, and iTRAQ labeling. Protein was extracted from male and female thirteen-lined ground squirrel quadriceps for each collection point. Equal amounts of protein were combined from one male and one female before tryptic digestion. The resulting peptides were iTRAQ labeled, and all samples were pooled for mass spectrometry analysis. This illustration depicts a single mass spec run, representing a single biological replicate for each collection point with technical replicates made from the APR and M-IBA samples. This process was performed three times for a total of three biological replicates.

matching a specific protein are then integrated to provide quantitative information for the protein. Comparisons were done between consecutive time points throughout the circannual cycle (Figure 1). A quantitative false discovery rate (FDR) of 2% was set by assigning a p -value threshold using the target-decoy method provided in the ProteinPilot Descriptive

Statistics Template (Sciex, Foster City, CA). The target-decoy method utilizes technical replicates (Figure 2) within a single MS/MS experiment to determine a p -value at which identical samples show an acceptable amount of difference (FDR of 2%). On the basis of this established FDR, proteins were considered differentially expressed within a single replicate if they had a p -value of <0.05 for the first and third replicates and a p -value below 0.001 for the second replicate. Because there is no standard method for averaging ratios and combining p -values across multiple MS runs, we considered protein abundances to be significantly different (using all three replicates) if at least two of the three replicates showed significance as previously stated and showed a similar change in abundance (upregulated or downregulated). Proteins that showed differential expression in conflicting directions were not used for further analysis. Protein lists were submitted to DAVID for broad functional analysis.

The identification of peptides corresponding to potential novel proteoforms was done largely using the platform Galaxy-P. Galaxy-P was used to filter out all peptides matching to known protein sequences from ground squirrel encoded by the NCBI genome. The remaining peptides, identified from RNaseq data, were filtered using BLAST-P to search against the NCBI thirteen-lined ground squirrel nonredundant database. Identifications made by BLAST-P were further filtered to account for percent of identical amino acids, number of gaps in query, and length of the query relative to the input. Resulting peptides were searched against the NCBI human database. Novel peptides identified from this process were checked for high-quality spectral matches using a Peptide Sequence Match Evaluator tool in Galaxy-P, and the protein sequences were aligned to ground squirrel and human sequences to visualize how the novel peptide differed from the known or predicted sequences.¹⁵ The workflows used in this study have been described in detail in a proteogenomic study of saliva.²²

RESULTS AND DISCUSSION

Role of Skeletal Muscle Plasticity in the Life Cycle of a Hibernator

The goal of this experiment was to identify proteomic transitions occurring in skeletal muscle that might explain certain tissue-specific and whole-body physiological transitions observed throughout the circannual cycle of this hibernator. A previous study in our lab developed a proteomic approach to identify proteins from nonmodel organisms that also used the thirteen-lined ground squirrel.²³ In this study, we employed iTRAQ-based tandem mass spectrometry (MS/MS) techniques to determine relative protein levels at six points throughout the year (Figure 1). In MS/MS runs 1, 2, and 3, respectively, there were 36 895, 40 833, and 34 813 spectra matched to peptide sequences. These spectra were used to identify 15 229, 16 586, and 16 753 distinct peptides. After searching these peptides against the NCBI-predicted protein database for the ground squirrel, our own database generated from high-throughput RNA-seq data, and a contaminant database, we identified 1055, 1335, and 1219 proteins across three separate MS/MS runs. Together, 1563 proteins were confidently identified. For differential expression analysis, we made comparisons between sequential collection points (Figure 1). Across all comparisons, 232 proteins met our criteria for differential expression (see Experimental Section). This approach recently identified a similar number of differentially expressed proteins in thirteen-

lined ground squirrel hearts.¹⁵ These 232 proteins were then functionally clustered using DAVID. Categories indicated by DAVID are consistent with previously described physiological transitions for hibernator skeletal muscle, such as changes in metabolic preference and fiber type (Figure 3).^{8,9,19,24}

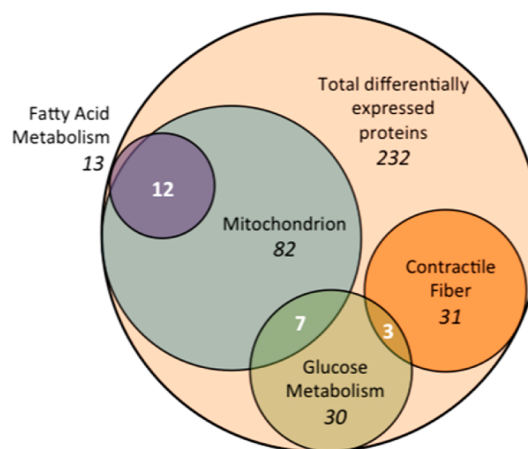


Figure 3. Major categorizations made by DAVID analysis of all differentially expressed proteins. Total number of proteins in a given category is represented with black numbers, whereas proteins shared between two categories are represented with white numbers.

Metabolic Transitions

The most notable transitions in protein abundance are consistent with previous findings that fatty acid oxidation is enhanced and glucose metabolism is reduced during the hibernation season in skeletal muscle.^{1,2} The comparison with the largest number of differentially expressed proteins was between M-IBA and APR, with 184 proteins. Despite the fact that these collection points are less than 1 month apart, this comparison has almost three times as many differentially expressed proteins than any other comparison. This supports the idea that the transition into the hibernation phenotype is a gradual one, occurring throughout the summer and fall, whereas the transition out of hibernation to an active and fed state is much more abrupt. The most notable fluctuations in metabolic proteins also occurred between the M-IBA and APR collection points (Figure 4). Relative to M-IBA, proteins related to glucose metabolism increase sharply, while fatty acid metabolism proteins decline at the APR collection point. During their final spring arousal, occurring between M-IBA and APR, the animals have access to carbohydrates for the first time in nearly 6 months. Thus, an increase in the enzymatic machinery necessary to derive energy from this new fuel source is important because they are recovering from the previous hibernation season and preparing for reproduction. Alternatively, the transition to efficiently metabolizing fatty acids is more gradual. As shown in Figure 4, proteins involved in fatty acid metabolism consistently have a positive ratio, indicating a gradual increase in abundance throughout most of the year. Similarly, proteins involved in glucose metabolism tend to have a negative ratio at the same comparisons, indicating a gradual decline. The comparison with the fewest differentially expressed proteins is TOR to J-IBA with 24 proteins. Because translation does not occur at T_b associated with TOR, IBAs are thought to be necessary for the production of proteins essential to the continuation of the hibernation phenotype.^{25,26} The majority of proteins with increased abundance at this comparison are

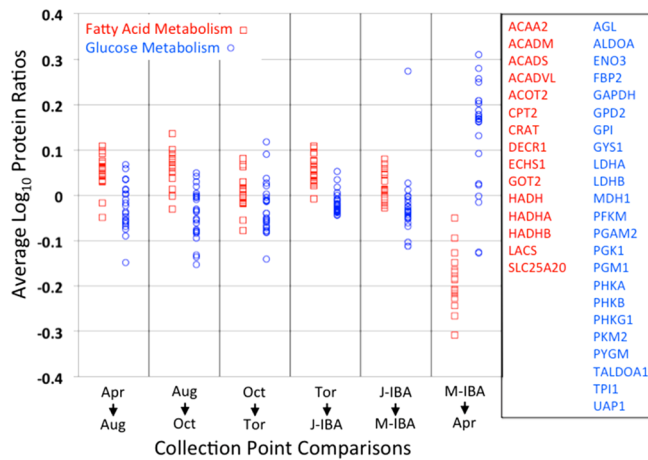


Figure 4. Abundance profile of metabolism-related proteins. All profiles charted are of proteins that are differentially expressed in at least one comparison. Red squares represent proteins involved in fatty acid metabolism. Blue circles represent proteins involved in glucose metabolism. Positive and negative ratios indicate an increase or decrease in protein abundance, respectively, from one time point to the next.

related to β -oxidation (HADHA, HADHB), the TCA cycle (FH, MDH1, SUCLA2, IDH3A, CS), and ATP synthesis (ATP5A1 and ATP5B). This reflects both the reliance of hibernating animals on fatty acid oxidation for making ATP as well as the importance of the IBAs for replenishing necessary proteins. In summary, these data provide valuable insight into the rate and timing of metabolic transitions occurring in the skeletal muscle of these hibernators.

Fiber-Type Transitions

Associated with these transitions in metabolic properties, we also see shifts in contractile proteins throughout the circannual cycle. Figure 5 shows the abundance of contractile proteins classified as fast-twitch, slow-twitch, or nonspecific isoforms. It should be pointed out that myosins comprise as much as 50% of the total protein of skeletal muscles and exist as either fast or

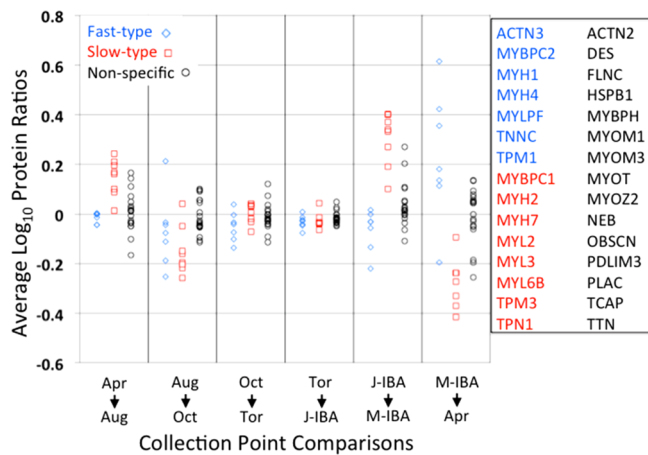


Figure 5. Abundance profile of contractile/structural proteins. All profiles charted are of proteins that are differentially expressed in at least one comparison. Blue diamonds represent protein isoforms consistent with a fast-type muscle. Red squares represent protein isoforms consistent with a slow-type muscle. Black circles represent proteins without specific fast or slow isoform types.

slow isoforms, so major shifts in these proteins will have a larger effect on muscle mass than others.²⁷ As with metabolism, the most abrupt transition occurs between the M-IBA and APR collection points, with increases in fast-twitch associated isoforms and a reduction in slow-twitch isoforms. This correlates with the fact that fast-twitch muscles use a more glycolytic metabolism and that these animals' muscles grow significantly upon spring refeeding.¹⁴ In contrast with the metabolic fluctuations, where we saw a gradual return to the hibernation phenotype, the contractile proteins show a much more variable abundance pattern, reflecting both changes in fiber-type abundance and overall muscle mass. APR to AUG shows an increase in muscle mass with increases in both fiber types. AUG to OCT, a period where these animals are greatly reducing their food intake and using shallow torpor bouts with increasing frequency,^{28,29} shows a reduction in both fiber types, likely indicating a reduction in muscle mass between these points. Fiber-type composition tends not to change through early hibernation but shows a surprising increase in abundance of slow-type isoforms between the J-IBA and M-IBA collection points. This transition supports a recent study demonstrating a reinvestment in muscle protein synthesis in preparation for spring arousal.¹⁴ These data suggest that these animals are actively growing muscle at a time when they have not eaten for at least 3 months and are mostly sedentary except for shivering thermogenesis and limited movement during IBAs.

Potential Roles of AMP Deaminase 1

The high abundance and metabolic demand of skeletal muscle necessitates the use of a strong negative feedback system in which this tissue can maintain energy balance in response to fluctuating energy demand and availability. The AMP/ATP ratio serves as a major signal of cellular energy status.^{30,31} During periods of high ATP utilization, this ratio is elevated.^{30,31} High AMP/ATP promotes the phosphorylation and activation of AMP-activated protein kinase (AMPK), which signals downstream processes aimed at increasing ATP production and decreasing ATP utilization.³² In response to acute energy deficit, AMPK maintains energy homeostasis through inhibiting protein synthesis and enhancing glucose and fatty acid uptake and utilization.³² For more chronic energy demand, AMPK has been implicated in increasing mitochondrial biogenesis through increased activity and activation of PGC-1 α , a transcriptional coactivator differentially expressed and activated during hibernation.^{20,33–35} A major regulator of the AMP/ATP ratio identified as being differentially expressed in our proteome is the protein AMP deaminase 1 (AMPD1) (Figure 7). AMPD1 catalyzes a rate limiting reaction in the main catabolic pathway of AMP to IMP, and thus its reduction would promote a higher AMP/ATP ratio during periods of rapid ATP hydrolysis.³⁶ These data demonstrate that the abundance of AMPD1 is significantly reduced preceding and during hibernation (Figure 8). This reduced ability to clear cellular AMP could lead to increased AMPK activity, especially during periods of muscle activity, which could induce many of the physiological transitions associated with hibernation including increased mitochondrial protein density (Figures 4 and 6), increased fatty acid metabolism (Figure 4),^{1,2} reduced muscle mass,¹⁴ and the fast to slow fiber-type transition (Figure 5),⁸ all of which occur at times congruent with reduced AMPD1 abundance.

Additionally, this decrease in AMPD1 during hibernation could reflect an alteration in the production of nitrogenous

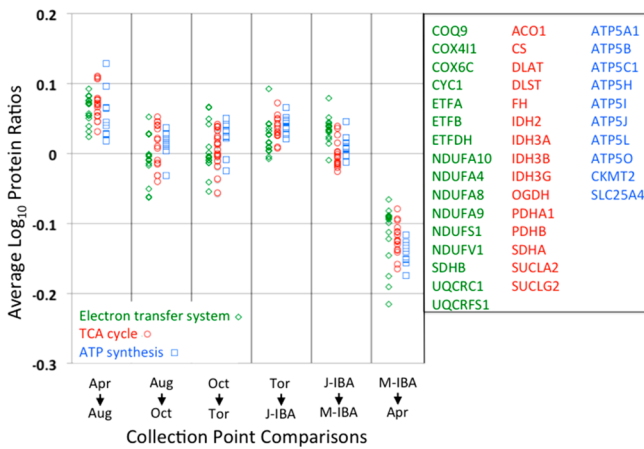


Figure 6. Abundance profile of mitochondrial proteins. Excludes metabolism proteins already shown in Figure 4. All profiles charted are of proteins that are differentially expressed in at least one comparison. Green diamonds represent proteins associated with the electron-transfer system. Red circles represent proteins involved in the TCA cycle. Blue squares represent proteins closely associated with ATP production, most of which are subunits of ATP synthase.

waste. During intense exercise, AMP is deaminated to IMP as a way of pulling the reaction catalyzed by adenylate kinase in the direction of making more ATP. As a consequence, tissue and blood levels of ammonia increase shortly after beginning exercise, reflecting this breakdown of AMP.^{37,38} Human individuals can, asymptotically, be heterozygous or homozygous for a mutation in AMPD1 that renders it catalytically inactive. Interestingly, these individuals show no increase in blood ammonia during or after exercise.³⁸ The reduced adenylate degradation in these individuals significantly reduces the amount of ammonia waste they produce during exercise.³⁸ These hibernators drink and urinate little, if at all, for the length of the hibernation season yet periodically need to activate their muscles to a high degree for shivering thermogenesis.¹⁰ Reducing the amount of nitrogenous waste produced during these exercise bouts greatly limits the amount of urine they need to produce.

Finally, reduced ability to clear cellular AMP may have another very active role in hibernation. With reduced ability to deaminate AMP to IMP, an alternate degradative pathway involves hydrolyzing AMP to adenosine.³⁷ During periods of high ATP utilization, such as shivering thermogenesis for IBAs, levels of muscle AMP and adenosine would be expected to spike.³⁷ Our previous work has shown that the transcript for the equilibrative nucleoside transporter 1 (SLC29A1) has significantly elevated expression during hibernation.²⁰ This transporter might allow the release of excess adenosine from the skeletal muscle into circulation.³⁹ Circulating adenosine has long been suspected as a major signal in the torpor-arousal cycle because it was demonstrated that adenine nucleotides or adenosine injections induce a hypometabolic state in mice with similarities to fasted daily torpor.^{40,41} Tissue-specific targets of adenosine might include the deactivation of nonshivering thermogenesis in brown adipose tissue (BAT). Previous work in our lab has shown an increase in the transcript of adenosine receptor ADORA1 in BAT during hibernation, the activation of which could shut down adenylate cyclase activity and the subsequent metabolism of fatty acids necessary for heat production.⁴² This would represent a signaling mechanism between the two main tissues responsible for rewarming and

maintenance of a normal euthermic T_b . As BAT produces heat in the initial phase of rewarming, it warms the muscles to the point that they can begin shivering thermogenesis. Because of the low levels of AMPD1, there would be greater potential to produce adenosine, which could enter circulation and activate ADORA1 in BAT. This would slow heat production in BAT as the animal reaches the desired T_b .

Further studies are underway to determine the role of AMPD1 in AMPK activation, reducing nitrogenous waste, and the potential effects on circulating adenylate levels, especially surrounding the intense shivering thermogenesis associated with rewarming.

Fibromodulin Helps Maintain Myogenic Potential in Myoblasts

Hibernator skeletal muscles have demonstrated delayed muscle regeneration during hibernation.⁴³ Interestingly, they delay regeneration without suffering increased fibrosis, as would happen in a typical mammal.^{43,44} Andres-Mateos et al. (2012) suggested that reduced levels of transforming growth factor- β (TGF- β) likely contribute to this phenomenon. TGF- β is a cytokine that is synthesized as an inactive complex that must be cleaved in the extracellular matrix (ECM) before binding to its receptor on the cell surface.⁴⁴ During myogenesis, its signaling determines the differentiation of fiber types while inhibiting muscle regeneration in adult muscle.⁴⁵ TGF- β signaling is thought to be involved in the inflammatory response to muscle damage, but persistent signaling will cause myogenic cells to differentiate into fibrotic cells instead of new muscle.⁴⁵ Various proteins of the ECM control TGF- β signaling by regulating cleavage to its active form or by sequestering it in the ECM to reduce its bioavailability.^{46–49} One such protein, fibromodulin (FMOD), increases significantly between AUG and OCT without a clear decrease, indicating a likely gradual decline in abundance (Figure 7). FMOD is known to bind and maintain both the active and inactive forms of TGF- β in the ECM, limiting its bioavailability.⁴⁸ Interestingly, it has also been shown play a role in the scarless repair of fetal skin.⁴⁹ Its role in hibernator skeletal muscle could be similar, with increased levels modulating TGF- β signaling, allowing for more of a fetal response to muscle damage, resulting in muscle regeneration instead of fibrosis. Further evidence of this mechanism presented in this paper is the increase in slow-type protein isoforms expressed late in the hibernation season. If there was a period of muscle regeneration occurring late in hibernation, within this fetal-like ECM, it is expected that gene and protein expression would reflect a slow-type muscle (Figure 5).⁴⁴ Because of TGF- β 's extensive roles in cellular growth and development, the regulation of its signaling through increased abundance of FMOD could play a significant role in the muscle maintenance seen during hibernation.

Multomics Analysis to Improve Genomic Annotation

Collection and analysis of high-throughput proteomic and RNaseq data from the same samples allowed us to identify specific amino acid sequences different from those predicted by automated genomic annotation. This proteogenomic method has proven particularly useful in nonmodel organisms, where genome annotation is typically less than ideal.¹⁵ Mass spectrometry runs 1, 2, and 3 identified 220, 214, and 241 peptides corresponding to novel proteoforms, respectively, with >95% confidence. 210 novel peptides were identified in two or more runs, with 99 being identified in all three runs. These 210 novel peptides represent 89 different proteins. This demon-

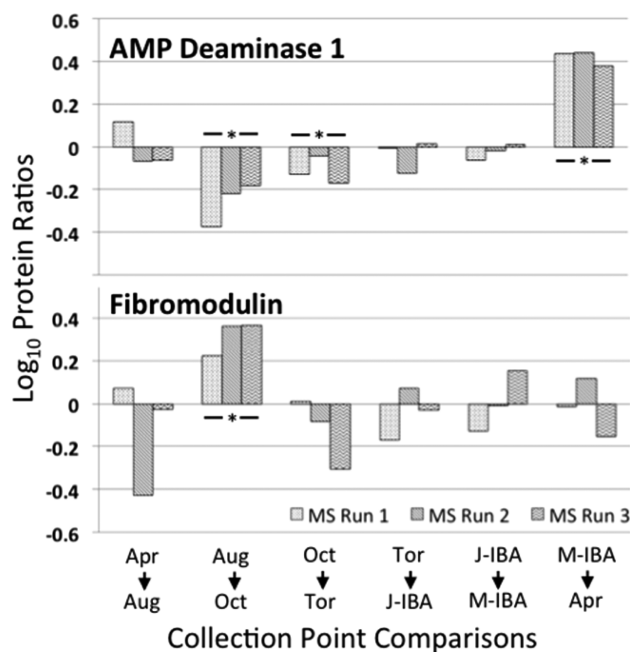


Figure 7. Relative protein abundance of AMPD1 and FMOD for six comparisons made throughout the circannual cycle. Ratios for each mass spec run are represented independently, with an asterisk indicating comparisons that fit our criteria for differential expression. AMP-deaminase 1 (AMPD1) shows significantly reduced abundance from AUG to OCT and from OCT to TOR while showing significantly increased abundance from M-IBA to APR. Fibromodulin (FMOD) has significantly increased abundance from AUG to OCT without any clear decrease, likely indicating a gradual decline, never showing significance.

strates the advantage of constructing a translated RNaseq database for proteomic analysis, as these peptides would have otherwise been unidentified. As previously reported in the ground squirrel heart, the majority of these peptides corresponding to novel proteoforms arise due to poor annotation of the genome.^{15,50} There were 77 peptides identified for 17 proteins that had no genomic prediction. Additionally, 16, 14, and 27 peptides were identified that, when also aligned to the human protein, exist before the predicted start site, after the predicted stop site, or within unpredicted exonic regions, respectively.

Other peptides were identified that had a specific number of amino acids different from the predicted protein. Seventeen peptides had 10 or more residues different from the predicted, likely indicating problems with genome annotation or new protein isoforms. Another 17 peptides had 6–9 amino acid differences from the predicted, representing proteins with high biological variability or poor annotation. Fifteen peptides had 2–5 differences from the predicted, while 24 peptides differed from their predicted sequence by a single amino acid, likely representing sequence variability between the populations used for genomic sequencing and those used in this study.

Proteome/Transcriptome Comparison

Another advantage to having both transcriptomic and proteomic screens from identical samples is the ability to interrogate basic biological questions such as the correlation between mRNA and protein abundance and the types of regulation that may be occurring at different points in the circannual cycle. As in previous studies, these data highlight the unreliability of transcriptomic data to predict protein

abundance.⁵¹ Of the differentially expressed transcripts that were also identified in the proteome, only 3.5 to 21.4% of them shared a similar expression pattern with their respective protein (Figure 8). This demonstrates a high degree of posttranscriptional regulation in determining protein levels.

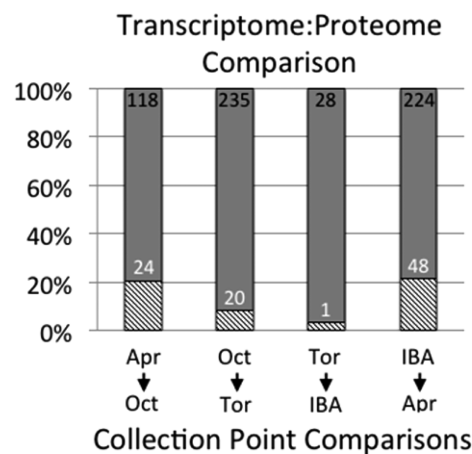


Figure 8. Differentially expressed transcripts and their protein products. Total number of differentially expressed transcripts with protein products identified in the proteome are indicated by the black numbers at the top of each bar. Total number of those proteins that show differential abundances similar to their respective transcripts are indicated by the white numbers, with the hatched bars indicating the percent of differentially expressed transcripts.

Our data also indicate that the level of posttranscriptional regulation may vary according to season or physiological transition. Although a similar number of differentially expressed transcripts were identified in the proteome in the Oct/Tor and IBA/Apr comparisons, the percentage of transcripts matching their respective protein abundance is more than double that in the latter comparison (Figure 8). This may indicate an increase in posttranscriptional regulation leading up to the hibernation season and a release from it following hibernation.

In conclusion, multiomics approaches offer a major advantage, especially to the study of nonmodel systems where genomic information may be sparse or inaccurate. While the depth of coverage in high-throughput proteomics is not yet to the level of transcriptomics, the disparities between the two and the higher biological relevance of protein data make it a valuable tool not only for testing specific hypotheses but also for the generation of new hypotheses, as was the goal of this study.

■ ASSOCIATED CONTENT

Supporting Information

The Supporting Information is available free of charge on the ACS Publications website at DOI: 10.1021/acs.jproteome.5b01138. The mass spectrometry proteomics data have been deposited to the ProteomeXchange Consortium via the PRIDE partner repository with the data set identifier PXD003188.

Supplemental Workbook 1: iTRAQ labeling strategy and differentially expressed proteins for sequential comparisons. (XLSX)

Supplemental Workbook 2.1: Protein Pilot protein summaries with denominators for each comparison made. (XLSX)

Supplemental Workbook 2.2: Protein Pilot protein summaries with denominators for each comparison made. (XLSX)

Supplemental Workbook 2.3: Protein Pilot protein summaries with denominators for each comparison made. (XLSX)

Supplemental Tables 1–3: Quality control data including PTMs, expected digestions, and missed cleavages for each of the three runs. (PDF)

AUTHOR INFORMATION

Corresponding Author

*E-mail: mandrews@d.umn.edu. Tel: 218-726-7271.

Notes

The authors declare no competing financial interest.

ACKNOWLEDGMENTS

This manuscript was improved by the helpful comments from Clair Hess. We thank LeeAnn Higgins and Todd Markowski for their role in proteomic data acquisition. This work was funded by NSF grant 1147079 for the Galaxy-P team, NIH Grant 1RC2HL101625-01 and USARMC contract W81XWH-11-0409 to M.T.A., and the University of Minnesota McKnight Presidential Endowment. We also acknowledge the Center for Mass Spectrometry and Proteomics and the Minnesota Supercomputing Institute for support.

REFERENCES

- (1) Andrews, M. T. Advances in Molecular Biology of Hibernation in Mammals. *BioEssays* **2007**, *29* (5), 431–440.
- (2) Carey, H. V.; Andrews, M. T.; Martin, S. L. Mammalian Hibernation: Cellular and Molecular Responses to Depressed Metabolism and Low Temperature. *Physiol. Rev.* **2003**, *83* (4), 1153–1181.
- (3) Zurlo, F.; Larson, K.; Bogardus, C.; Ravussin, E. Skeletal Muscle Metabolism Is a Major Determinant of Resting Energy Expenditure. *J. Clin. Invest.* **1990**, *86* (5), 1423–1427.
- (4) Fluck, M. Functional, Structural and Molecular Plasticity of Mammalian Skeletal Muscle in Response to Exercise Stimuli. *J. Exp. Biol.* **2006**, *209* (12), 2239–2248.
- (5) Pieter de Lange, Moreno, M.; Silvestri, E.; Lombardi, A.; Goglia, F.; Lanni, A. Fuel Economy in Food-Deprived Skeletal Muscle: Signaling Pathways and Regulatory Mechanisms. *FASEB J.* **2007**, *21* (13), 3431–3441.
- (6) Schiaffino, S.; Reggiani, C. Fiber Types in Mammalian Skeletal Muscles. *Physiol. Rev.* **2011**, *91* (4), 1447–1531.
- (7) Stevenson, E. J.; Giresi, P. G.; Koncarevic, A.; Kandarian, S. C. Global Analysis of Gene Expression Patterns during Disuse Atrophy in Rat Skeletal Muscle. *J. Physiol.* **2003**, *551* (1), 33–48.
- (8) Nowell, M. M.; Choi, H.; Rourke, B. C. Muscle Plasticity in Hibernating Ground Squirrels (*Spermophilus lateralis*) Is Induced by Seasonal, but Not Low-Temperature, Mechanisms. *J. Comp. Physiol., B* **2011**, *181* (1), 147–164.
- (9) Xu, R.; Andres-Mateos, E.; Mejias, R.; MacDonald, E. M.; Leinwand, L. A.; Merriman, D. K.; Fink, R. H. A.; Cohn, R. D. Hibernating Squirrel Muscle Activates the Endurance Exercise Pathway despite Prolonged Immobilization. *Exp. Neurol.* **2013**, *247*, 392–401.
- (10) Postnikova, G. B.; Tselikova, S. V.; Kolaeva, S. G.; Solomonov, N. G. Myoglobin Content in Skeletal Muscles of Hibernating Ground Squirrels Rises in Autumn and Winter. *Comp. Biochem. Physiol., Part A: Mol. Integr. Physiol.* **1999**, *124* (1), 35–37.
- (11) Andres-Mateos, E.; Brinkmeier, H.; Burks, T. N.; Mejias, R.; Files, D. C.; Steinberger, M.; Soleimani, A.; Marx, R.; Simmers, J. L.; Lin, B.; Finanger Hedderick, E.; Marr, T. G.; Lin, B. M.; Hourdé, C.; Leinwand, L. A.; Kuhl, D.; Föller, M.; Vogelsang, S.; Hernandez-Diaz, I.; Vaughan, D. K.; Alvarez de la Rosa, D.; Lang, F.; Cohn, R. D. Activation of Serum/glucocorticoid-Induced Kinase 1 (SGK1) Is Important to Maintain Skeletal Muscle Homeostasis and Prevent Atrophy. *EMBO Mol. Med.* **2013**, *5* (1), 80–91.
- (12) Lee, K.; Park, J. Y.; Yoo, W.; Gwag, T.; Lee, J. W.; Byun, M. W.; Choi, I. Overcoming Muscle Atrophy in a Hibernating Mammal despite Prolonged Disuse in Dormancy: Proteomic and Molecular Assessment. *J. Cell. Biochem.* **2008**, *104* (2), 642–656.
- (13) Brooks, N. E.; Myburgh, K. H.; Storey, K. B. Myostatin Levels in Skeletal Muscle of Hibernating Ground Squirrels. *J. Exp. Biol.* **2011**, *214* (Pt 15), 2522–2527.
- (14) Hindle, A. G.; Otis, J. P.; Epperson, L. E.; Hornberger, T. A.; Goodman, C. A.; Carey, H. V.; Martin, S. L. Prioritization of Skeletal Muscle Growth for Emergence from Hibernation. *J. Exp. Biol.* **2015**, *218* (2), 276–284.
- (15) Vermillion, K. L.; Jagtap, P.; Johnson, J. E.; Griffin, T. J.; Andrews, M. T. Characterizing Cardiac Molecular Mechanisms of Mammalian Hibernation via Quantitative Proteogenomics. *J. Proteome Res.* **2015**, *14*, 4792.
- (16) Sheynkman, G. M.; Johnson, J. E.; Jagtap, P. D.; Shortreed, M. R.; Onsongo, G.; Frey, B. L.; Griffin, T. J.; Smith, L. M. Using Galaxy-P to Leverage RNA-Seq for the Discovery of Novel Protein Variations. *BMC Genomics* **2014**, *15* (1), 703.
- (17) Boekel, J.; Chilton, J. M.; Cooke, I. R.; Horvatovich, P. L.; Jagtap, P. D.; Käll, L.; Lehtio, J.; Lukasse, P.; Moerland, P. D.; Griffin, T. J. Multi-Omic Data Analysis Using Galaxy. *Nat. Biotechnol.* **2015**, *33* (2), 137–139.
- (18) Jagtap, P. D.; Blakely, A.; Murray, K.; Stewart, S.; Kooren, J.; Johnson, J. E.; Rhodus, N. L.; Rudney, J.; Griffin, T. J. Metaproteomic Analysis Using the Galaxy Framework. *Proteomics* **2015**, *15*, 3553–3565.
- (19) Smith, L. M.; Kelleher, N. L.; et al. Proteoform: A Single Term Describing Protein Complexity. *Nat. Methods* **2013**, *10* (3), 186–187.
- (20) Vermillion, K. L.; Anderson, K. J.; Hampton, M.; Andrews, M. T. Gene Expression Changes Controlling Distinct Adaptations in the Heart and Skeletal Muscle of a Hibernating Mammal. *Physiol. Genomics* **2015**, *47* (3), 58–74.
- (21) Yang, F.; Shen, Y.; Camp, D. G.; Smith, R. D. High-pH Reversed-Phase Chromatography with Fraction Concatenation for 2D Proteomic Analysis. *Expert Rev. Proteomics* **2012**, *9* (2), 129–134.
- (22) Jagtap, P. D.; Johnson, J. E.; Onsongo, G.; Sadler, F. W.; Murray, K.; Wang, Y.; Sheynkman, G. M.; Bandhakavi, S.; Smith, L. M.; Griffin, T. J. Flexible and Accessible Workflows for Improved Proteogenomic Analysis Using the Galaxy Framework. *J. Proteome Res.* **2014**, *13* (12), 5898–5908.
- (23) Russeth, K. P.; Higgins, L.; Andrews, M. T. Identification of Proteins from Non-Model Organisms Using Mass Spectrometry: Application to a Hibernating Mammal. *J. Proteome Res.* **2006**, *5* (4), 829–839.
- (24) Hindle, A. G.; Karimpour-Fard, A.; Epperson, L. E.; Hunter, L. E.; Martin, S. L. Skeletal Muscle Proteomics: Carbohydrate Metabolism Oscillates with Seasonal and Torpor-Arousal Physiology of Hibernation. *AJP Regul. Integr. Comp. Physiol.* **2011**, *301* (5), R1440–R1452.
- (25) van Breukelen, F.; Martin, S. L. Translational Initiation Is Uncoupled from Elongation at 18 Degrees C during Mammalian Hibernation. *Physiology* **2001**, *281* (5), R1374–R1379.
- (26) van Breukelen, F.; Sonenberg, N.; Martin, S. L. Seasonal and State-Dependent Changes of eIF4E and 4E-BP1 during Mammalian Hibernation: Implications for the Control of Translation during Torpor. *Am. J. Physiol. Regul. Integr. Comp. Physiol.* **2004**, *287* (2), R349–R353.
- (27) Bielewicz, J.; Zanin, M. E.; Galbani, A.; Carraro, U. Contractile Proteins Content of Long Term Permanent Denervated Human Muscle after Functional Electrical Stimulation. *Basic Appl. Myol* **2004**, *14* (2), 83–86.
- (28) Russell, R. L.; O'Neill, P. H.; Epperson, L. E.; Martin, S. L. Extensive Use of Torpor in 13-Lined Ground Squirrels in the Fall

prior to Cold Exposure. *J. Comp. Physiol., B* **2010**, *180* (8), 1165–1172.

(29) Schwartz, C.; Hampton, M.; Andrews, M. T. Hypothalamic Gene Expression Underlying Pre-Hibernation Satiety. *Genes, Brain Behav.* **2015**, *14* (3), 310–318.

(30) Hardie, D. G.; Salt, I. P.; Hawley, S. A.; Davies, S. P. AMP-activated protein kinase: an ultrasensitive system for monitoring cellular energy charge. *Biochem. J.* **1999**, *338*, 717–722.

(31) Hardie, D. G. Minireview: The AMP-Activated Protein Kinase Cascade: The Key Sensor of Cellular Energy Status. *Endocrinology* **2003**, *144* (12), 5179–5183.

(32) Hardie, D. G.; Ross, F. a.; Hawley, S. a. AMPK: A Nutrient and Energy Sensor That Maintains Energy Homeostasis. *Nat. Rev. Mol. Cell Biol.* **2012**, *13* (4), 251–262.

(33) Zong, H.; Ren, J. M.; Young, L. H.; Pypaert, M.; Mu, J.; Birnbaum, M. J.; Shulman, G. I. AMP Kinase Is Required for Mitochondrial Biogenesis in Skeletal Muscle in Response to Chronic Energy Deprivation. *Proc. Natl. Acad. Sci. U. S. A.* **2002**, *99* (25), 15983–15987.

(34) Lee, W. J.; Kim, M.; Park, H.-S.; Kim, H. S.; Jeon, M. J.; Oh, K. S.; Koh, E. H.; Won, J. C.; Kim, M.-S.; Oh, G. T.; Yoon, M.; Lee, K.-U.; Park, J.-Y. AMPK Activation Increases Fatty Acid Oxidation in Skeletal Muscle by Activating PPAR α and PGC-1. *Biochem. Biophys. Res. Commun.* **2006**, *340* (1), 291–295.

(35) Jäger, S.; Handschin, C.; St.-Pierre, J.; Spiegelman, B. M. AMP-Activated Protein Kinase (AMPK) Action in Skeletal Muscle via Direct Phosphorylation of PGC-1 α . *Proc. Natl. Acad. Sci. U. S. A.* **2007**, *104* (29), 12017–12022.

(36) Chapman, A. G.; Atkinson, D. E. Stabilization of Adenylate Energy Charge by the Adenylate Deaminase Reaction. *J. Biol. Chem.* **1973**, *248* (23), 8309–8312.

(37) Plaideau, C.; Lai, Y.-C.; Kviklyte, S.; Zanou, N.; Löfgren, L.; Andersén, H.; Vertommen, D.; Gailly, P.; Hue, L.; Bohlooly-Y, M.; Hallén, S.; Rider, M. H. Effects of Pharmacological AMP Deaminase Inhibition and Ampd1 Deletion on Nucleotide Levels and AMPK Activation in Contracting Skeletal Muscle. *Chem. Biol.* **2014**, *21* (11), 1497–1510.

(38) Norman, B.; Sabina, R. L.; Jansson, E. Regulation of Skeletal Muscle ATP Catabolism by AMPD1 Genotype during Sprint Exercise in Asymptomatic Subjects. *J. Appl. Physiol.* **2001**, *91* (1), 258–264.

(39) Beal, P. R.; Yao, S. Y. M.; Baldwin, S. A.; Young, J. D.; King, A. E.; Cass, C. E. The Equilibrative Nucleoside Transporter Family, SLC29. *Pfluegers Arch.* **2004**, *447* (5), 735–743.

(40) Zhang, J.; Kaasik, K.; Blackburn, M. R.; Lee, C. C. Constant Darkness Is a Circadian Metabolic Signal in Mammals. *Nature* **2006**, *439* (19), 340–343.

(41) Swoap, S. J.; Rathvon, M.; Gutilla, M. AMP Does Not Induce Torpor. *Am. J. Physiol. Regul. Integr. Comp. Physiol.* **2007**, *293* (1), R468–R473.

(42) Hampton, M.; Melvin, R. G.; Andrews, M. T. Transcriptomic Analysis of Brown Adipose Tissue across the Physiological Extremes of Natural Hibernation. *PLoS One* **2013**, *8* (12), e85157.

(43) Andres-Mateos, E.; Mejias, R.; Soleimani, A.; Lin, B. M.; Burks, T. N.; Marx, R.; Lin, B.; Zellars, R. C.; Zhang, Y.; Huso, D. L.; Marr, T. G.; Leinwand, L. a.; Merriman, D. K.; Cohn, R. D. Impaired Skeletal Muscle Regeneration in the Absence of Fibrosis during Hibernation in 13-Lined Ground Squirrels. *PLoS One* **2012**, *7* (11), e48884.

(44) Piersma, B.; Bank, R. A.; Boersema, M. Signaling in Fibrosis: TGF- β , WNT, and YAP/TAZ Converge. *Front. Med.* **2015**, *2* (September), 1–14.

(45) Burks, T. N.; Cohn, R. D. Role of TGF- β Signaling in Inherited and Acquired Myopathies. *Skeletal Muscle* **2011**, *1* (1), 19.

(46) Roberts, A. B.; McCune, B. K.; Sporn, M. B. TGF- β : Regulation of Extracellular Matrix. *Kidney Int.* **1992**, *41* (3), 557–559.

(47) Zheng, Z.; Jian, J.; Zhang, X.; Zara, J. N.; Yin, W.; Chiang, M.; Liu, Y.; Wang, J.; Pang, S.; Ting, K.; Soo, C. Reprogramming of Human Fibroblasts into Multipotent Cells with a Single ECM Proteoglycan, Fibromodulin. *Biomaterials* **2012**, *33* (24), 5821–5831.

(48) Hildebrand, A.; Romaris, M.; et al. Interaction of the Small Interstitial Proteoglycans Biglycan, Decorin and Fibromodulin with Transforming Growth Factor Beta. *Biochem. J.* **1994**, *302*, 527–534.

(49) Soo, C.; Hu, F. Y.; Zhang, X.; Wang, Y.; Beanes, S. R.; Lorenz, H. P.; Hedrick, M. H.; Mackool, R. J.; Plaas, a.; Kim, S. J.; Longaker, M. T.; Freymiller, E.; Ting, K. Differential Expression of Fibromodulin, a Transforming Growth Factor-Beta Modulator, in Fetal Skin Development and Scarless Repair. *Am. J. Pathol.* **2000**, *157* (2), 423–433.

(50) Nesvizhskii, A. I. Proteogenomics: Concepts, Applications and Computational Strategies. *Nat. Methods* **2014**, *11* (11), 1114–1125.

(51) Griffin, T. J. Complementary Profiling of Gene Expression at the Transcriptome and Proteome Levels in *Saccharomyces Cerevisiae*. *Mol. Cell. Proteomics* **2002**, *1* (4), 323–333.